Evaluation of Torque Measurement Surrogates as Applied to Grip Torque and Jaw Angle Estimation of Robotic Surgical Tools

John J. O'Neill, Trevor K. Stephens, and Timothy M. Kowalewski

***Abstract*—The estimation of grip force for surgical tools such as the da Vinci has been shown to be valuable in possible applications such as haptics, tissue identification, and surgical training. Successful estimation attempts have been previously demonstrated, but utilize customized sensors; this letter aims to provide an estimate considering only typical sensor streams already present in commercially available surgical robots. The objective of this letter is to evaluate three proximal-end torque surrogate methods in their abilities to estimate distal-end states. The estimates are compared with previously reported results found in literature and the percent difference between the customized sensor approach and previous standards is reported. The most effective surrogates for proximal-end torque were commanded motor current and measured motor current. The jaw angle estimate resulted in 0.37 degree root mean square error, and the distal-end torque estimate resulted in 4.42 mNm RMSE, which compares favorably to existing literature approaches.**

***Index Terms*—Surgical robotics: Laparoscopy, medical robots and systems, AI-based methods, perception for grasping and manipulation.**

I. BACKGROUND

THE utilization of sensory information for analytics and estimation is becoming more readily adopted across a wide variety of applications. These applications include soil quality estimation for improved farming [1], road condition monitoring for smoother driving [2], and anomaly estimation in ultraprecision machining to reduce rework rates [3]. Despite adoption across these diverse application areas, one area which acutely underutilizes sensory data is in robotic surgery. Robots are inherently equipped with sensors to accomplish proper control, yet these sensor streams are potentially underutilized for additional benefits. Such benefits include realization of haptic feedback to surgeons [4]–[6], automation of surgical subtasks [7], [8], as well as classification of *in-vivo* tissues during surgical procedures [9], [10]. One challenge in utilizing the existing available sensory data from surgical robots is the indirect use of raw sensor measurements to approximate true measurements at the distal gripping end. This is because sensors are not placed at the point of grasping, but rather are situated on the proximal side, separated by a complicated cable-pulley mechanism at varying tension. To alleviate this problem, several estimation techniques have been presented to transform available proximal-end measurements to useful distal-end estimates [11]–[13]. Estimation usually emphasizes grip force of a surgical jaw.

As of yet, these estimation techniques have been limited to laboratory settings and as such, require that some limiting assumptions be made. In [11], [12], the authors assume to have full access to input torque measurements. Additionally, in [13], the da Vinci tool model was only derived in the quasi-static case. Additionally, in [14] it is established that different roll pitch and yaw angles of the wrist can have a large impact on grip force. Currently, surgical robots are not equipped with torque sensors on the proximal end and are most often operated under dynamic conditions. Understanding estimation accuracy under more-realistic conditions is valuable.

II. METHODS

The research objective herein is to evaluate three available analogues for proximal-end torque: measured motor current, motor commanded current, and gearbox differential. Experiment 1 consists of predicting proximal end torque utilizing these surrogates to establish a baseline for torque estimation. Experiment 1 compares a linear fit and a neural network to map each surrogate method to the proximal end torque sensor. This experiment does not involve the surgical tool. Experiment 2 consists of predicting distal end torque comparing two methods: staged approach and end-to-end approach. The staged approach uses the estimate of proximal end torque from experiment 1 as in intermediate step in estimating distal-end torque. The end-to-end approach uses a neural network to estimate distal-end torque and jaw angle directly, bypassing the need for a torque sensor altogether. Experiment 3 employs the end-to-end approach for all three torque surrogates on a training dataset containing varying roll, pitch, and yaw (RPY) angles. This dataset is used to test the estimation validity in more realistic jaw orientations experienced in surgery, where the degrees of freedom are rarely constrained.

Manuscript received February 20, 2018; accepted June 3, 2018. Date of publication June 22, 2018; date of current version July 9, 2018. This letter was recommended for publication by Associate Editor D. Stoyanov and Editor K. Masamune upon evaluation of the reviewers' comments. This work was supported in part by the Army Research Laboratory and was accomplished under Cooperative Agreement Number W911NF-14-2-0035 and in part by the National Science Foundation Graduate Research Fellowship under Grant 00039202. *(Corresponding author: John J. O'Neill.)*

The authors are with the Department of Mechanical Engineering, University of Minnesota, Minneapolis, MN 55455 USA (e-mail: oneil463@umn.edu; steph594@umn.edu; timk@umn.edu).

Digital Object Identifier 10.1109/LRA.2018.2849862

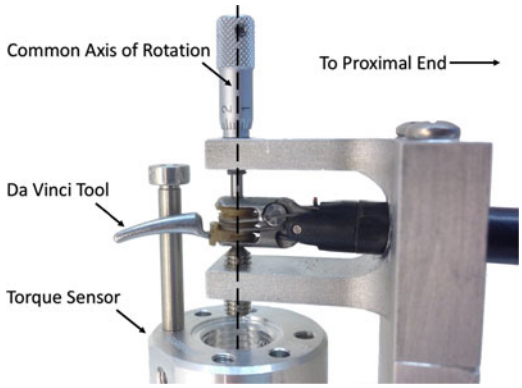

Fig. 1. Distal end hardware for data collection depicting common axis of rotation between the torque sensor and da Vinci tool jaw.

In summary, the main contributions of this work are as follows:

- Assess the proximal torque estimation ability of three different torque surrogate methods, which are more readily available on existing surgical robots than torque sensors (Experiment 1).
- Assess the estimation ability of the same torque surrogate methods to estimate distal-end grip force and jaw angle of a da Vinci surgical tool using a neural network (Experiment 2).
- Assess the estimation ability of the end-to-end approach using all three torque surrogate methods in the presence of varying roll, pitch, and yaw (Experiment 3)
- Quantify estimation errors and compare with existing literature.

The letter is outlined in the following manner: Section II details the methods used in completing the three experiments; Section III reports numerical results of the experiments; Section IV discusses the implications from using each surrogate method and compares these results with existing literature values.

A. Hardware

The hardware used for data collection consisted of a distal-end ground truth measurement device as shown in Figure 1 and a proximal end da Vinci tool driver shown in Figure 2. The distal end is comprised of a FUTEK TFF325 reaction torque sensor (FUTEK Advanced Sensor Technology, Inc., Irvine, California) and optical encoder (not pictured) to measure torque and jaw angles about the common axis of rotation. The da Vinci tool is pinned in place at this axis of rotation with a micrometer head and cone point set screw. Further details of the distal end hardware can be found in [15]. The proximal end da Vinci tool driver consists of a Maxon servomotor (Maxon Motor, Sachseln, Switzerland) driving one of the spindles of a da Vinci Si Maryland Grasper tool (Figure 2-i) directly. The motors have a reduced backlash 35:1 planetary gearhead, and a 4,096 count per turn encoder. An additional 8,192 counts per revolution CUI AMT 102 encoder (CUI Inc., Tualatin, OR) and a FUTEK TFF325 reaction torque sensor (FUTEK Advanced Sensor Technology, Inc., Irvine, California) were placed on the shaft directly connected to the spindle.

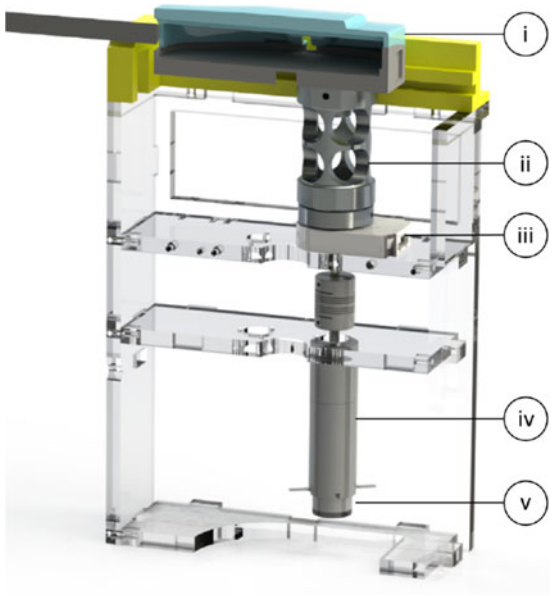

Fig. 2. A section view of the hardware with annotations depicting key elements on the back-end: i) da Vinci Si Maryland Grasper ii) Futek reaction torque sensor iii) CUI encoder post gearbox iv) DCX 19 S Maxon motor v) ENX16 EASY Maxon encoder.

The motors were controlled and the data logged by a 32 bit Teensy 3.5 microcontroller (PJRC, Sherwood OR, USA), which allowed for the creation of a time-synchronized, proximal-to-distal-end database of sensor streams. A Maxon ESCON Module 24/2 Servo Controller was used to control the motor in current control mode with an analog output of the Teensy microcontroller commanding a motor current, which was controlled with current feedback. For each time step, running at 1 KHz, the commanded current, measured current, measured torque, and post- and pre-gearbox positions were recorded as time-synced data points as part of the proximal end measurements, along with the sensors described in [15] for the distal end measurements. Both proximal and distal sensors were connected to the same microcontroller, allowing all sensors to be time-synchronized.

The position was measured directly using the encoders present at the proximal end. The following four sensor types were used to measure, directly or indirectly, the torque at the proximal end:

1) Ground Truth. Torque Sensor: The FUTEK torque sensor (Figure 2-ii) provides a ground truth for torque at the back end of the tool. However, as this is not available in commercial surgical robots, it was only used in this work to provide a reference point to evaluate other torque estimation methods.

2) Torque Analogue A. Measured Current: The first surrogate method for torque is via measured current. The Maxon motor (Figure 2-iv) has a motor driver with a feedback loop around motor current, and can provide the current measurement as an analog output. This has been shown to be approximately linearly proportional to the output torque of a brushed DC motor.

3) Torque Analogue B. Commanded Current: The second surrogate method for torque is commanded current. If the

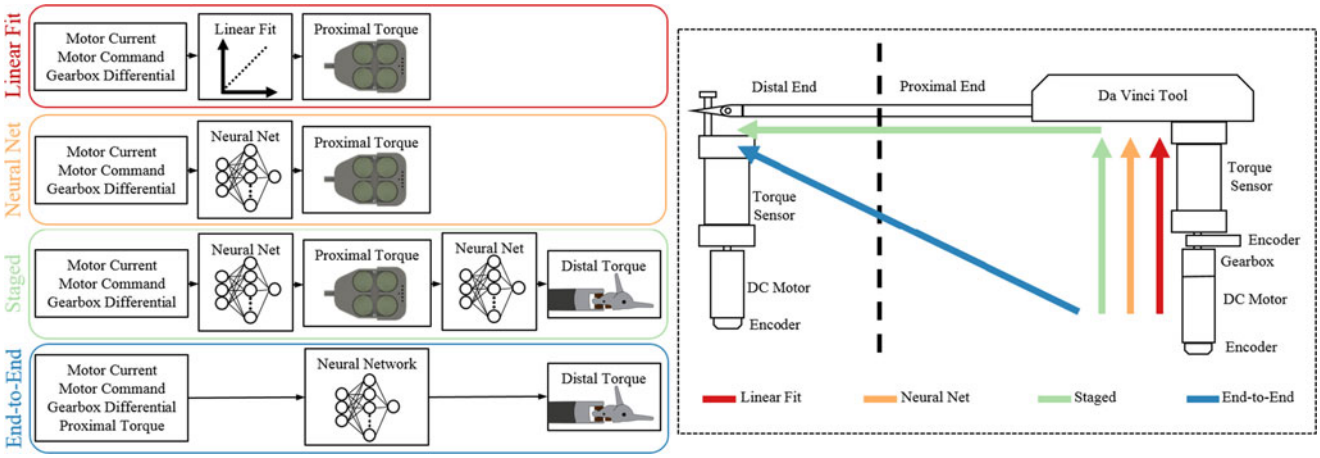

Fig. 3. Conceptual diagram depicting the four experimental methods along with a conceptual schematic showing the sensor input-output relationships for each experiment.

measured motor current is not available, the command sent to the motor driver could be used. For example, it is already available from the da Vinci Logger from Intuitive Surgical. The commanded current is anticipated to less accurately portray the actual motor current when compared with measured current due to slight inefficiencies in the motor controller.

4) Torque Analogue C. Gearbox Differential: The third surrogate method for torque is gearbox differential. If no other estimates of torque are available, the torque could possibly be estimated by the difference between a pre-gearbox encoder (Figure 2-v) and a post-gearbox encoder (Figure 2-iii). As the torque increases, the gearbox components will flex, which can be measured by the difference in encoder values compared to the expected gear ratio. In this setup, the gear ratio is 1:35 and the ratio of encoder resolutions is 1:2. Therefore, the expected ratio of the encoder values is 1:17.5. Any deviation from this expected ratio could theoretically be used to calculate the torque in the system.

5) Combined Torque Analogues: In addition to each of the three torque analogues individually, using all three simultaneously was also tested. This was tested because in a real-world situation more than one of the three torque analogues may be available, so it was desired to test whether the combination of the torque analogues could outperform each one individually.

B. Data Collection

The dataset for experiments 1 and 2 consisted of 50 total runs comprised of 20 seconds of sinusoidal grasps. The 50 runs included ten different power levels (10% to 100% at 10% increments) and five different frequencies (0.1 Hz to 0.5 Hz at 0.1 Hz increments). The permutations of these grasps resulted in a total of 1,000,000 data points collected at 1 kHz.

The dataset for experiment 3 introduced non-fixed roll, pitch, and yaw angles. The roll varied between -90 to 90° and pitch between -60 to 60°. Additionally, the sinusoidal grasp start points were shifted from the neutral yaw position ranging from -90 to 30°. These coordinate frames are depicted in Figure 4. To facilitate a reasonably-sized dataset, frequency was

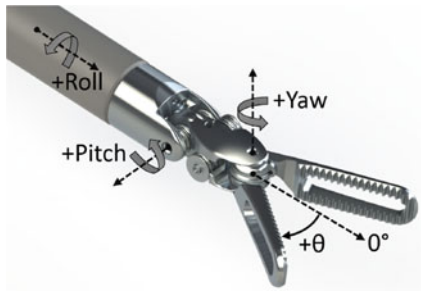

Fig. 4. Coordinate frame notation of the da Vinci EndoWrist depicting the roll and pitch notations used in experiment 3.

intentionally constant throughout experimentation at 0.3 Hz, and power levels ranged from 10% to 40%. This yielded a total of 2,800,000 data points collected at 1 kHz. All datasets are hosted at github.com/MRDLab/mis-tool-characterization.

The power levels provide resistive torque at the jaw to simulate the various reaction forces experienced in surgical procedures. These power levels correspond to the commanded current, and 100% power yields approximately 250 mNm of applied torque from the distal motor. This motor was judiciously selected to produce resistive grip forces which encapsulate reported grip forces on typical da Vinci Si tools from literature. Assuming a measured moment arm of 12mm, our resistive force would equate to a range of 2.1 N to 20.8 N. Literature suggests that the mean grip force in the neutral position ranges across tools from 6.01 N-16.3 N in [14], and 3.78 N-19.9 N in [6], with the reported grip force from a Maryland bipolar forceps being 7.77 N. The selected motor fully encapsulates this range of tools.

C. Data Preprocessing

As only the closing forces were considered relevant, the data were segmented to remove any negative or near-zero velocities. Additionally, the first and last second of each run were removed in order to remove any startup or shutdown effects. This left a total of 260,581 data points for the training and evaluation

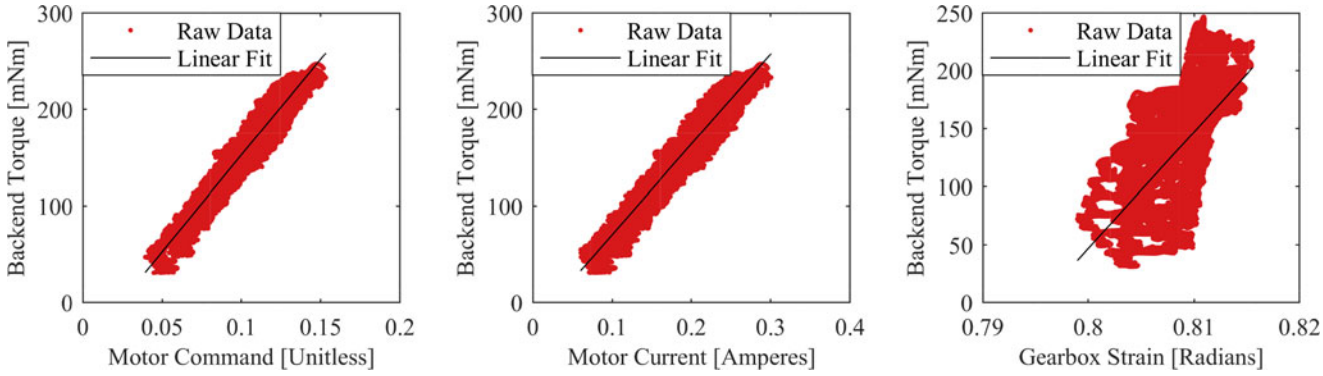

Fig. 5. Experiment 1: Linear approximation of backend torque for three torque surrogates.

for experiments 1 and 2. For experiment 3 a total of 962,936 data points remained after this preprocessing step. The data were filtered in order to provide smoother data by applying a 3rd order Butterworth low pass filter with a 3dB cutoff of 50 Hz. The derivatives were taken with a noise-robust numerical differentiation method as described by Holoborodko (11th order, non-causal numerical differentiator) [16].

D. Neural Network Estimation

For all neural network estimation used in this work the same network structure was utilized. The neural network consisted of 30 nodes per layer and a single hidden layer due to Kolmogorovs theorem, which states that a single hidden layer can approximate any non-linear function arbitrarily well [17]. For all experimentation the inputs to the neural network were at the very least position, velocity, and a chosen torque surrogate, with the exception of the combined test, where not just one but all three torque surrogates were used as input nodes. For experiment 3, the additional inputs of measured pitch and roll spindle angles were used in the neural network. Training was accomplished using Bayesian regularization backpropagation [18], [19] as implemented in the Matlab Neural Network Toolbox (The MathWorks, Inc., Natick, Massachusetts). A training dataset was partitioned from 85% of the dataset, leaving 15% of the data as a test set which remains blind to the training procedure. The training data was randomly chosen from the entire range of the dataset. The outputs of the neural network were proximal-end torque for experiment 1, and jaw angle and distal-end torque for experiments 2 and 3.

E. Experiment 1: Proximal Torque Estimation

Experiment 1 compared a baseline for torque estimation using a linear fit to torque estimation via a neural network. The fit line was compared to the measured torque sensor values and the error was computed. The mean absoluter error (MAE), 95th percentile of that error, and root mean absolute error (RMSE) were all computed and tabulated. Pearson's Correlation (R) was used to measure goodness of fit to linearity. For secondary analysis purposes, Spearman rho (ρ) was used to measure monotonicity.

Each surrogate method was used individually as an input to a neural network along with position and velocity to estimate torque, and the same metrics were used, other than Spearman rho (ρ) and Pearson's Correlation (R). This experiment was done without any distal sensors; it was purely to show different experimental approaches of each surrogate method's ability to estimate torque on the proximal end.

F. Experiment 2: Distal Torque and Position Estimation

Experiment 2 evaluated the three surrogate methods of torque by comparing using the estimation results from the neural networks of experiment 1 as an input to another neural network to an end-to-end neural network to predict the distal-end torque and jaw angle. This neural network was trained with the torque values from the proximal end torque sensor, but tested with torque estimates from each of the three surrogate methods. The neural network outputs both jaw angle and distal-end torque; these estimates were compared with ground truth measurements taken at the distal end and their errors were plotted and tabulated. For the end-to-end neural network, the proximal torque sensor was unused.

A diagram summarizing the four variables of the first two experiments and showing the input-output sensor mapping for these experiments is shown in Figure 3.

G. Experiment 3: Estimation With Varying Pitch and Roll

Experiment 3 evaluated the end-to-end approach in the presence of varying roll, pitch, and yaw angles. The pitch and roll angles were allowed to vary in their specified ranges one at a time, while testing the possible yaw angles. Accordingly, two sets of estimates were produced: varying pitch and varying roll. These estimates were compared with ground truth measurements taken at the distal end and their errors were plotted and tabulated.

III. RESULTS

A. Experiment 1: Proximal Torque Estimation

The results from Experiment 1's linear estimation of proximal torque are shown in Figure 5 and Table I. Both measured motor current and commanded motor current provide the best accuracies with motor command providing a slightly better accuracy with an RMSE of 12.18 mNm. The gearbox differential

TABLE I
EXPERIMENT 1: PROXIMAL TORQUE [MNM]

		MAE	95^{th} Pctl	RMSE	R	ρ
Linear	Motor Command	10.03	22.94	12.18	0.97	0.97
	Motor Current	10.06	23.26	12.26	0.97	0.97
	Gearbox Strain	33.91	76.30	40.53	0.60	0.62
Neural Net	Motor Command	4.37	11.54	5.69		
	Motor Current	4.47	11.72	5.80		
	Gearbox Strain	11.54	36.89	16.90		
	All 3 Sensors	3.82	10.04	4.94		

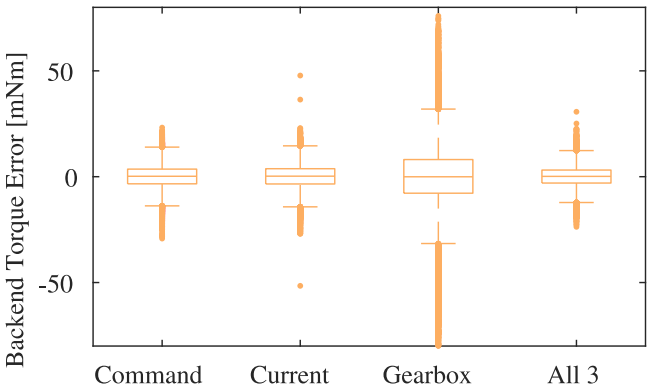

Fig. 6. Experiment 1: Proximal neural network estimation error of backend torque.

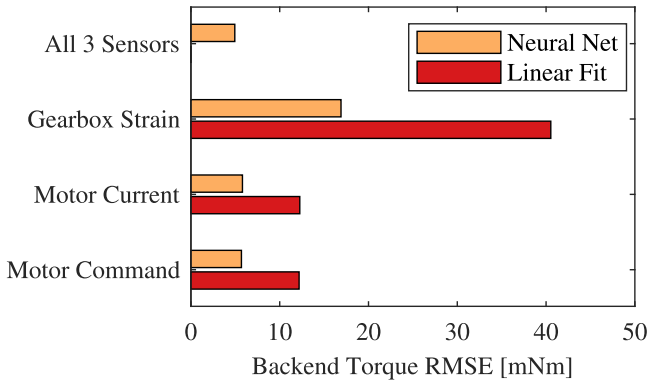

Fig. 7. Comparison of backend torque RMSE for experiment 1 comparing a linear fit and neural network fit.

method provides a significantly worse estimate of torque with an RMSE of 40.53 mNm.

The Pearson's correlation was low for the gearbox differential method, at 0.60, showing that a linear fit is not well suited. Additionally, the Spearman's rho is also poor, at 0.62, showing that any monotonic relationship (linear or otherwise) is also not well suited.

The neural network estimation of proximal torque is shown in Figure 6, where both the measured and commanded motor current provide similar accuracies with commanded current producing the lowest RMSE of the three at 5.69 mNm. This equates to approximately 53% reduction in error from the linear model to neural network approach in estimating torque. The gearbox differential estimation provides a significantly worse estimate of torque with an RMSE of 16.90 mNm. When all three torque analogue sensors were used, the RMSE was further reduced to 4.94 mNm. The tabulated results are shown in Table I.

TABLE II
EXPERIMENT 2: DISTAL POSITION [DEG]

		Mean Abs Err	95^{th} Pctl	RMSE
Staged	Motor Command	0.28	0.73	0.36
	Motor Current	0.29	0.74	0.37
	Gearbox Strain	0.65	2.26	1.00
	All 3 Sensors	0.25	0.64	0.32
End-to-End	Motor Command	0.28	0.74	0.37
	Motor Current	0.30	0.77	0.38
	Gearbox Strain	0.69	2.33	1.00
	All 3 Sensors	0.28	0.73	0.36
	Torque Sensor	0.13	0.33	0.17

TABLE III
EXPERIMENT 2: DISTAL TORQUE [MNM]

		Mean Abs Err	95^{th} Pctl	RMSE
Staged	Motor Command	3.28	9.49	4.49
	Motor Current	3.37	9.71	4.59
	Gearbox Strain	7.87	25.03	11.65
	All 3 Sensors	2.92	8.32	3.94
End-to-End	Motor Command	3.33	9.00	4.42
	Motor Current	3.42	9.28	4.72
	Gearbox Strain	8.42	24.91	12.09
	All 3 Sensors	2.86	7.60	3.75
	Torque Sensor	1.20	3.39	1.78

B. Experiment 2: Distal Torque and Position Estimation

For jaw angle estimation using the neural network from Experiment 1 to estimate proximal torque, the estimates of distal-end jaw angle utilizing the commanded motor current and measured motor current provide similar accuracy (Figure 8). Using motor command yields an estimation with the lowest RMSE of the three at 0.36 degrees. The gearbox differential method provides a significantly worse estimate with an RMSE of 1.00 degrees. When all three torque analogue sensors were used, the RMSE was 0.32 degrees. The tabulated results are shown in Table II.

As shown in Figure 9 the estimates of jaw torque at the distal end using the neural network from experiment 1 utilizing the commanded and measured motor current provide similar accuracies, with motor command resulting in a slightly lower RMSE of 4.49 mNm. The gearbox differential method provides a significantly worse estimate with an RMSE of 11.65 mNm. When all three torque analogue sensors were used, the RMSE was 3.94 mNm. The tabulated results are shown in Table III.

As shown in Figure 10, the estimates of jaw angle from a single neural net utilizing both commanded and measured motor current provide similar accuracies. The motor command provides the best estimation with 0.37 degrees RMSE. The gearbox differential estimation provides a significantly worse estimate with an RMSE of 1.00 degrees. When all three torque analogue sensors were used, the RMSE was 0.36 degrees. These compare

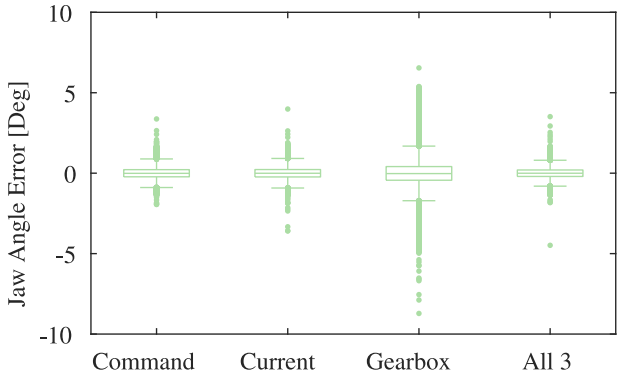

Fig. 8. Experiment 2: Distal neural network estimation error of jaw angle.

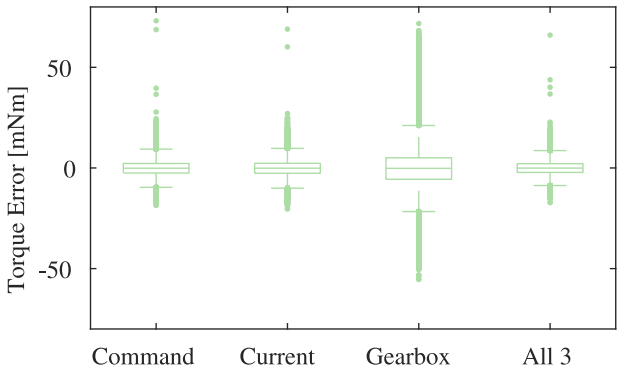

Fig. 9. Experiment 2: Distal neural network estimation error of end effector torque.

to an RMSE of 0.17 degrees when the torque sensor is used as an input to the neural net. The tabulated results are shown in Table II.

As shown in Figure 11, the estimates of distal-end torque from a single neural net utilizing both the commanded and measured motor current provide similar accuracies; the motor command provides the best estimation with 4.42 mNm RMSE. The gearbox differential method provides a significantly worse estimate with an RMSE of 12.09 mNm. When all three torque analogue sensors were used, the RMSE was 3.75 mNm. These compare to an RMSE of 1.78 mNm when the torque sensor is used as an input to the neural net. The tabulated results are shown in Table III.

C. Experiment 3: Estimation With Varying Pitch and Roll

As shown in Figure 14, the estimates of jaw angle using an end-to-end neural net shows better accuracy during varied pitch than during varied roll. Of the three toque surrogates, the motor command provides the best estimation for pitch, with 0.35 degrees and motor current provides the best estimation for roll with 0.49 degrees RMSE respectively. These compare to an RMSE of 0.17 degrees for pitch and 0.34 degrees for roll when the torque sensor is used as an input to the neural net. The tabulated results are shown in Table IV

As shown in Figure 15 the estimates of distal-end torque using an end-to-end neural net shows better accuracy during varied

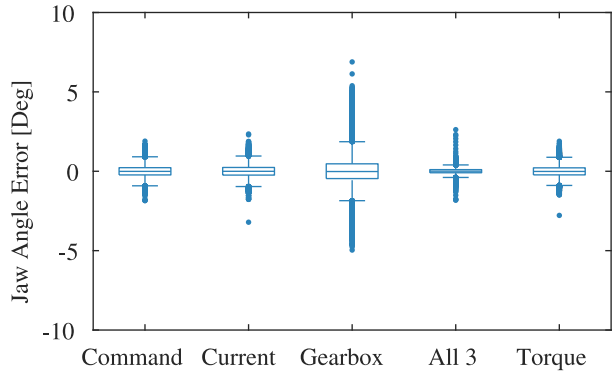

Fig. 10. Experiment 2: Full neural network estimation error of jaw angle.

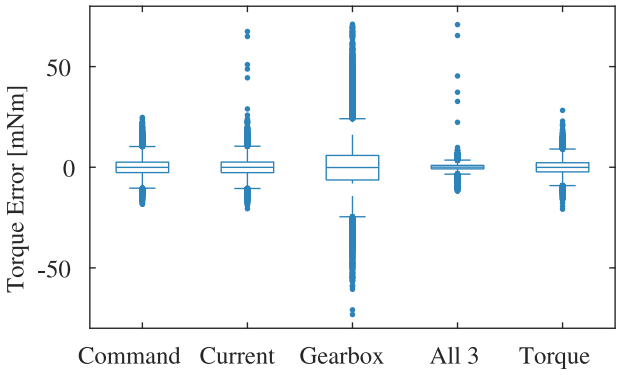

Fig. 11. Experiment 2: Full neural network estimation error of end effector torque.

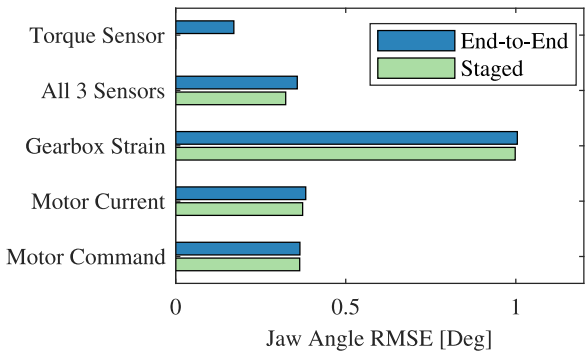

Fig. 12. Experiment 2 RMSE of jaw angle.

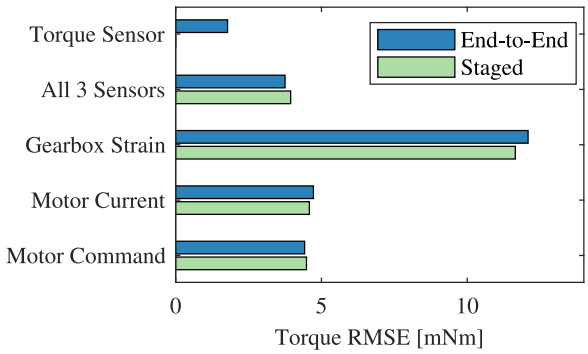

Fig. 13. Experiment 2 RMSE of end effector torque.

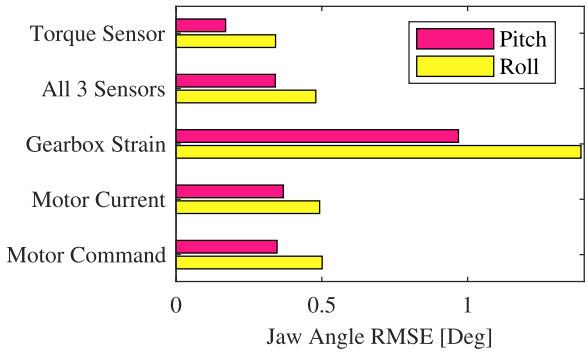

Fig. 14. Experiment 3 RMSE of jaw angle.

TABLE IV
EXPERIMENT 3 RPY: JAW ANGLE [DEG]

		Mean Abs Err	95^{th} Pctl	RMSE
Varied Pitch	Motor Command	0.26	0.70	0.35
	Motor Current	0.28	0.75	0.37
	Gearbox Strain	0.70	2.12	0.97
	All 3 Sensors	0.25	0.68	0.34
	Torque Sensor	0.13	0.34	0.17
Varied Roll	Motor Command	0.37	0.99	0.50
	Motor Current	0.36	0.98	0.49
	Gearbox Strain	1.11	2.69	1.39
	All 3 Sensors	0.35	0.95	0.48
	Torque Sensor	0.23	0.67	0.34

TABLE V
EXPERIMENT 3 RPY: TORQUE [MNM]

		Mean Abs Err	95^{th} Pctl	RMSE
Varied Pitch	Motor Command	3.12	8.38	4.16
	Motor Current	3.31	9.02	4.41
	Gearbox Strain	8.63	25.41	11.77
	All 3 Sensors	2.86	7.37	3.71
	Torque Sensor	1.64	4.69	2.24
Varied Roll	Motor Command	5.50	15.42	7.91
	Motor Current	5.62	15.38	7.95
	Gearbox Strain	14.64	34.55	18.08
	All 3 Sensors	5.37	14.76	7.67
	Torque Sensor	3.80	12.63	6.31

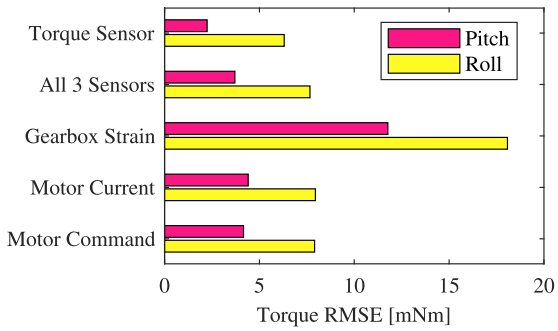

Fig. 15. Experiment 3 RMSE of end effector torque.

pitch than during varied roll. Of the three toque surrogates, the motor command provides the best estimation for both pitch and roll, with 4.16 mNm and 7.91 mNm RMSE respectively. These compare to an RMSE of 2.24 mNm for pitch and 6.31 mNm for roll when the torque sensor is used as an input to the neural net. The tabulated results are shown in Table I.

IV. DISCUSSION

The experimental results show that both measured and commanded current are feasible torque surrogates and provide sufficient estimation results over the tested dynamic range assuming proper techniques are applied (i.e., not a linear mapping). The gearbox differential method was confirmed to be a poor surrogate for torque as evident from a low Pearson's correlation and Spearman's rho. The combination of all three sensors did outperform each sensor individually, but did not provide much benefit beyond the motor current and motor command. The two successful surrogates for torque provide a very low jaw angle estimation error (0.37 degrees RMSE), and establish a benchmark for jaw angle estimation error as to our knowledge there is no existing work showing this estimation. The estimates for jaw torque are comparable with existing literature. Li and Hannaford [11] report a best-case grip force error of 0.07 Newtons for grasps with a peak value of approximately 1 Netwon. This equates to a 7% error normalized against peak grasp force. Our estimation method yields a converted grip force error of 0.37 Newtons when using a measured 12 mm moment arm. This is for grasps with a peak value of approximately 11.1 Newtons. This results in a 3.5% error when normalized against peak force. Although these comparisons may not be perfect, they give a good idea that even against the previously reported best-case scenario our results compare favorably.

The Experiment 1 linear results show that even for measured motor current—often assumed to be linearly related to torque—the nonlinearities of the system provide noticeable error. However, they do have a somewhat predictable dependency on position and velocity, allowing the neural net to provide a greatly improved accuracy. This change can clearly be seen in Figure 7 where for each torque analogue the neural net reduces the error by at least half. This provides evidence that a linear estimate between current and torque can be significantly improved by including position and velocity states in the estimate.

The results from experiment 2's staged approach, using the network from experiment 1, provided some of the lowest errors (see Tables II and III), but the experimental technique employed still requires the use of a proximally-located torque sensor in the training process. The torque sensor is not required for implementation on-line, but the need for a proximally-located torque sensor during the process may be limiting. The end-to-end neural network approach allowed a simpler training scheme by avoiding the proximal end torque sensor altogether. This experimental technique represents the most translational option to a surgical robot, as it only relies on readily available torque surrogate measurement methods for both training and on-line implementation with negligible loss in accuracy.

The experiment 2 staged results slightly outperformed the end-to-end results, which can be seen in Figure 12 for position and Figure 13 for torque. This shows that an intermediate ground truth helps during training even if unavailable while running. However, the practicality of an end-to-end system outweighs the minimal gains seen in the staged system; therefore, we propose the end-to-end methodology as the preferred technique. While the gearbox differential estimation failed to outperform the other methods in any experiment, not all motor controllers provide current feedback or current control, so the gearbox differential estimation may be the only option. In this scenario, RMSE of around 1 degree and 12 mNm for jaw angle and torque, respectively, should be expected.

Experiment 3 varied roll, pitch, and yaw angles within the dataset and the results show that the methods presented here still provide useful accuracy even with expected cross-talk between degrees of freedom. The accuracies in pitch are essentially the same as those from experiment 2, which implies that the pitch changes can easily be incorporated into the neural network. However, variations in roll did show a noticeable decrease in accuracy, where the RMSE for jaw angle increased approximately 25% and the RMSE for torque estimation approximately doubled. This occurs to a similar degree even for the torque sensor, so it does not seem related to the torque surrogate choice. This implies that roll imparts more cross-talk, possibly due to the fact that roll causes the cables to twist as the shaft rotates relative to the base. This result aligns with that found by [14], which showed the highest variation in grip force occurred with a nonzero roll. The lower accuracy for roll implies that if this method is to be used, roll should be minimized if possible.

A limitation of this study is that different types of tool were not tested, as well as the fact that tool-to-tool and tool lifetime variation were not taken into account, and further study should investigate these effects. A benefit of this method is its fast execution. The neural network, due to only having one hidden layer and 30 nodes, can be evaluated in less than a microsecond, allowing for very low latency applications, such as haptics. The sensor readings and filtering would add some time, but at the very least 1 kHz should be achievable, as this study was performed at this rate, and this would be fast enough for smooth haptic feedback.

These results show that there is value in the raw data created by surgical robots, regardless of the make or model, so long as there is some sort of torque analogue. The typical errors to be expected are herein quantified. Regardless of the method used, the accuracy is sufficient to provide a useful estimate of the torque being applied, which could be applied to training, haptics, or even tissue property identification to make surgery safer and more effective. A lack of a proximal torque sensor should not inhibit the collection and use of robotic minimally invasive surgery data.

ACKNOWLEDGMENT

The views and conclusions contained in this document are those of the authors and should not be interpreted as representing the official policies, either expressed or implied, of the Army Research Laboratory or the U.S. Government. The U.S. Government is authorized to reproduce and distribute reprints for Government purposes notwithstanding any copyright notation herein. Any opinion, findings, and conclusions or recommendations expressed in this material are those of the authors and do not necessarily reflect the views of the National Science Foundation. The full dataset is hosted at github.com/MRDLab/mis-tool-characterization.

REFERENCES

[1] S. Ivanov, K. Bhargava, and W. Donnelly, "Precision farming: Sensor analytics," *IEEE Intell. Syst.*, vol. 30, no. 4, pp. 76–80, Jul./Aug. 2015.

[2] A. Ghose, P. Biswas, C. Bhaumik, M. Sharma, A. Pal, and A. Jha, "Road condition monitoring and alert application: Using in-vehicle smartphone as internet-connected sensor," in *Proc. IEEE Int. Conf. Pervasive Comput. Commun. Workshops*, 2012, pp. 489–491.

[3] O. F. Beyca, P. K. Rao, Z. Kong, S. T. Bukkapatnam, and R. Komanduri, "Heterogeneous sensor data fusion approach for real-time monitoring in ultraprecision machining (UPM) process using non-parametric Bayesian clustering and evidence theory," *IEEE Trans. Autom. Sci. Eng.*, vol. 13, no. 2, pp. 1033–1044, Apr. 2016.

[4] A. M. Okamura, "Haptic feedback in robot-assisted minimally invasive surgery," *Current Opinion Urology*, vol. 19, no. 1, pp. 102–107, 2009.

[5] O. Van der Meijden and M. Schijven, "The value of haptic feedback in conventional and robot-assisted minimal invasive surgery and virtual reality training: A current review," *Surgical Endoscopy*, vol. 23, no. 6, pp. 1180–1190, 2009.

[6] M. C. Lee, C. Y. Kim, B. Yao, W. J. Peine, and Y. E. Song, "Reaction force estimation of surgical robot instrument using perturbation observer with smcspo algorithm," in *Proc. IEEE/ASME Int. Conf. Adv. Intell. Mechatron.*, 2010, pp. 181–186.

[7] B. Kehoe *et al.*, "Autonomous multilateral debridement with the raven surgical robot," in *Proc. IEEE Int. Conf. Robot. Autom.*, 2014, pp. 1432–1439.

[8] A. Murali *et al.*, "Learning by observation for surgical subtasks: Multilateral cutting of 3-D viscoelastic and 2-D orthotropic tissue phantoms," in *Proc. IEEE Int. Conf. Robot. Autom.*, 2015, pp. 1202–1209.

[9] R. Dockter, J. O'Neill, T. Stephens, and T. Kowalewski, "Feasibility of tissue classification via da vinci endowrist surgical tool," in *Proc. Hamlyn Symp. Med. Robot.*, 2016, pp. 64–65.

[10] T. K. Stephens, Z. C. Meier, R. M. Sweet, and T. M. Kowalewski, "Tissue identification through back end sensing on da Vinci endowrist surgical tool," *J. Med. Devices Tech. Brief*, vol. 9, no. 3, 2015, Art no. 030939.

[11] Y. Li and B. Hannaford, "Gaussian process regression for sensorless grip force estimation of cable-driven elongated surgical instruments," *IEEE Robot. Autom. Lett.*, vol. 2, no. 3, pp. 1312–1319, Jul. 2017.

[12] Y. Li, M. Miyasaka, M. Haghighipanah, L. Cheng, and B. Hannaford, "Dynamic modeling of cable driven elongated surgical instruments for sensorless grip force estimation," in *Proc. IEEE Int. Conf. Robot. Autom.*, 2016, pp. 4128–4134.

[13] F. Anooshahpour, I. G. Polushin, and R. V. Patel, "Quasi-static modeling of the da Vinci instrument," in *Proc. IEEE Int. Conf. Intell. Robots Syst.*, 2014, pp. 1308–1313.

[14] C. Lee *et al.*, "A grip force model for the da Vinci end-effector to predict a compensation force," *Med. Biol. Eng. Comput.*, vol. 53, no. 3, pp. 253–261, 2015.

[15] N. Kong, T. Stephens, J. O'Neill, and T. Kowalewski, "Design of a portable dynamic calibration instrument for da Vinci si tools," in *Proc. ASME Des. Med. Devices Conf.*, 2017, Art. no. 3519.

[16] P. Holoborodko, "Smooth noise robust differentiators," 2008. [Online]. Available: http://www.holoborodko.com/pavel/numerical-methods/numerical-derivative/smoo th-low-noise-differentiators/

[17] R. Hecht-Nielsen, "Kolmogorov's mapping neural network existence theorem," in *Proc. Int. Conf. Neural Netw.*, 1987, pp. 11–14.

[18] D. J. MacKay, "A practical Bayesian framework for backpropagation networks," *Neural Comput.*, vol. 4, no. 3, pp. 448–472, 1992.

[19] F. D. Foresee and M. T. Hagan, "Gauss-newton approximation to Bayesian learning," in *Proc. IEEE Int. Conf. Neural Netw*, 1997, vol. 3, pp. 1930–1935.